Global Journal of Researches in Engineering: I
Numerical Methods
Volume 20 Issue 1 Version 1.0 Year 2020
Type: Double Blind Peer Reviewed International Research Journal
Publisher: Global Journals
Online ISSN: 2249-4596 & Print ISSN: 0975-5861

# Finite and Numerical Simulations Applied in Tailor Welded Blank

By Wellington Augusto dos Santos, Etiene Pereira de Andrade,
Guilherme Souza Assunção & Gilmar Cordeiro da Silva
*Pontifícia Universidade Católica de Minas Gerais*

*Abstract-* The increase in economic and technological competitiveness means that the automobile industry seeks constant innovation in its production methods and processes, in order to produce lighter, safer and more efficient vehicles. Products with greater mechanical resistance, better conformability, thickness combinations of plates / materials are sought with a focus on reducing mass and increasing the rigidity of the vehicle body. In this scenario, Tailor Welded Blank (TWB), which is a top welding technique (by unconventional processes) of sheets of different specifications (materials, thicknesses and / or coatings), appears as a solution, as it allows localized distribution of mechanical properties, mass, optimizing the relationship between structural rigidity and the total weight of the vehicle body. The great challenge of this technique is to combine two processes with completely different demands, welding and mechanical forming. Due to the complexity of forming TWBs, the use of simulations has been widely adopted. In this review, different results of the numerical simulation methods used for a Tailor Welded Blank are compared, focusing on the details and the influence of the parameters used.

*Keywords:* *numerical simulation; tailor welded blank.*

*GJRE-I Classification:* *FOR Code: 010301*


*Strictly as per the compliance and regulations of:*

# Finite and Numerical Simulations Applied in Tailor Welded Blank

Wellington Augusto dos Santos [α], Etiene Pereira de Andrade [σ], Guilherme Souza Assunção [ρ] & Gilmar Cordeiro da Silva [ω]

*Abstract-* The increase in economic and technological competitiveness means that the automobile industry seeks constant innovation in its production methods and processes, in order to produce lighter, safer and more efficient vehicles. Products with greater mechanical resistance, better conformability, thickness combinations of plates / materials are sought with a focus on reducing mass and increasing the rigidity of the vehicle body. In this scenario, Tailor Welded Blank (TWB), which is a top welding technique (by unconventional processes) of sheets of different specifications (materials, thicknesses and / or coatings), appears as a solution, as it allows localized distribution of mechanical properties, mass, optimizing the relationship between structural rigidity and the total weight of the vehicle body. The great challenge of this technique is to combine two processes with completely different demands, welding and mechanical forming. Due to the complexity of forming TWBs, the use of simulations has been widely adopted. In this review, different results of the numerical simulation methods used for a Tailor Welded Blank are compared, focusing on the details and the influence of the parameters used.

*Keywords: numerical simulation; tailor welded blank.*

## I. Introduction

Tailor Welded Blank (TWB) is the combination of two or more metal sheets joined through the welding process, as shown in FIG. 1.There is possible to get a part with different materials, thicknesses, mechanical properties and coatings. This process leverages the global market in several sectors and especially the automotive market, due to the advantage of reducing production costs, weight and improving the structural performance of the vehicle. [1,2,3,8].

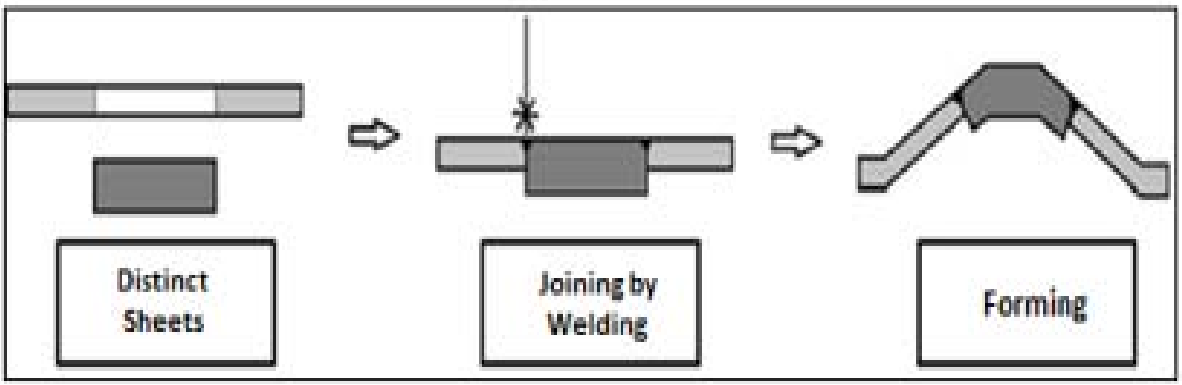


*Source: (Adapted from ZHANG et al, 2016.)*

*Figure 1:* Tailor Welded Blank principle

The patent this technique happened in 1964, been utilized on a large scale only in the late 1980s. In 1992, their application in the automotive industry stood out rightly, for its versatility [2,3,8]. The development of TWB technique shown in figure 2, enabled application in several parts in the car body, what that made possible the increment of resistance and mechanical rigidity according to the need of the vehicle and the behavior of the added part [1,2,3,8].

*Author α: Pontifícia Universidade Católica de Minas Gerais, Belo Horizonte/MG, Brasil. e-mail: augustowellington@ymail.com*
*Author σ: Bolsista de Desenvolvimento Tecnológico Industrial-DTI - Conselho Nacional de Desenvolvimento Cientifico e Tecnológico-CNPQ, Belo Horizonte/MG, Brasil.*
*e-mail: andrade.etiene@hotmail.com*
*Author ρ: Universidade Federal de Minas Gerais, Belo Horizonte/MG, Brasil. e-mail: guilhermeassuncao@hotmail.com*
*Author ω: Pontifícia Universidade Católica de Minas Gerais, Belo Horizonte/MG, Brasil. e-mail: gilmarcord@gmail.com*

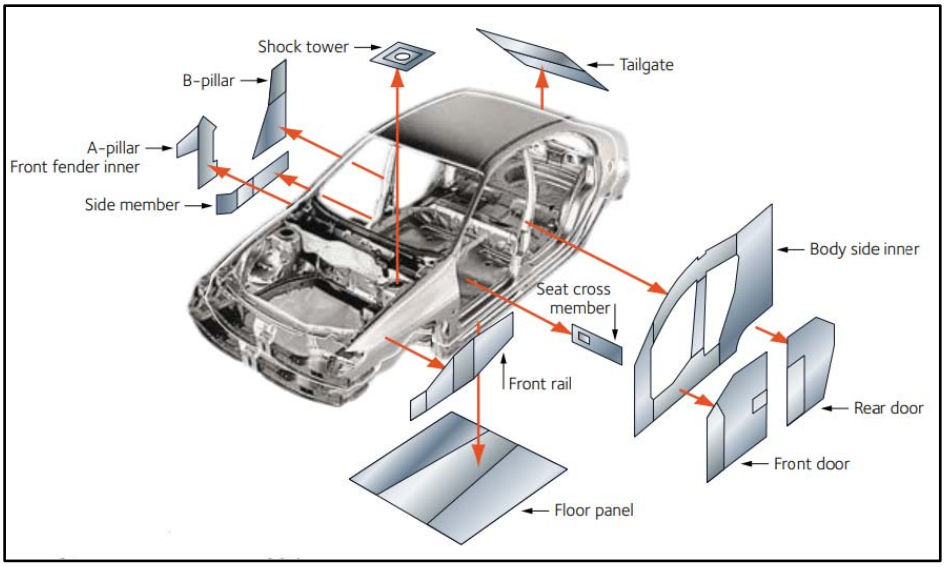


*Source: (Adapted from the Arcelor Mittal Europe catalog, p.7).*

*Figure 2:* Parts of a Car body with the application of Tailor Welded Blank

However, despite the advantages conferred by the use of TWB, their application can be considered complex, involving several variables and some complications. The most common problems are splits in the weld region, injurious levels of residual stresses, reduced formability in and displacement of the weld line during forming [2,3,8].

To avoid the occurrence of failures, some adjustments are made to the dies and recently was worked finite element analysis simulations in computer. However, given the complexities of modeling conventional of TWBs, the levels of correlation are not always the best. Numerical modeling of TWBs is more complicated than the modeling of conventional sheet metal forming processes. The great difficulty in performing the numerical modeling in the TWBs conformation is due to the mechanical properties caused by the welding process, and the non-uniformity of the base materials. [3,4,5].

This paper aims to provide an overview of the use of numerical modeling techniques for different simulations in TWBS, listing the advantages and disadvantages in industrial application, as well as the challenges and research activities.

## II. Numerical Simulation Methods in Sheet Forming

The appearance of the finite element methods (FEM) occurred in the aerospace industry in the early 1950s, as a powerful numerical tool for solving mathematical engineering and physics problems, improvement the numerical resolution of a system of partial differential equations. One of the reasons why the FEM has been successful since the beginning of its formulation is its basic concept of discretization that produces many simultaneous algebraic equations that are generated and solved with the help of computers [6,7,8].

Due to the complexity of the sheet forming process, mainly in the deep-drawing operation, a fact, which led the engineers and designers, incorporate the FEM to development, seen the need to reduce the time and costs in the modelling of a new project. [6,8,55,62,63].

The representations of the effects of the contours of the elements in the sheets forming must be considered for permanent deformations and major changes in the geometry of the product. For this, it is necessary to use interpolation functions, which are curves built from known values, which in this case are the degrees of freedom of the element nodes. [6,7,9,55,62].

During the stamping of a product, the blank is subjected to a complex historical deformation and varied boundary conditions. Because of this loading history, the theory should describe the deformation of the blank that can be discretized as bi or three-dimensional. Three different classes of elements can be used in the printing simulation: MEMBRANE, SHELL and SOLID [6,9].

The membrane elements have three degrees of freedom of translation per node, in the direction that two nodes are tangent and a force is normal to knot. The orientation of the normal force at the node is determined by averaging the normal forces adjacent to the element. The geometry of the sheet is adjusted through the contact of the tools. However, this method is not recommended for calculating elastic return (spring back), as it does not accurately represent the simulated values [7,9].

The shell elements have a knot with five degrees of freedom: three of translation for the two tangent vectors and the normal vector, and two rotations with the tangent vectors on the axis of rotation. The shell element is an element capable of calculating bending and has membrane characteristics. Loading in flat and perpendicular directions is allowed. All shell element formulations have an arbitrary number of integration points along the thickness of the sheet. It is recommended for all stamping operations, but it does not express accuracy for sheets of high thickness [6,7,9].

The 3D or solid elements represent all degrees of freedom and the results of a simulation with this element allow an accurate visualization of stresses and strains through the thickness and with precise spring back data. Results of a simulation with solid elements help to visualize the material's behavior in problematic regions. The disadvantage of this method is the processing time, as there are solid elements in the thickness that generate a model with many more elements, which does not happen when we use the shell elements [7,9].

## III. Numerical Modeling Methods in Tailor Welded Blanks

Numerical modeling in TWBs is more complicated than modeling of conventional sheet metal forming processes, mainly due to the change in mechanical and elastoplastic properties caused by the welding process and the difference in thickness between the base materials [5,10,11,12,61].

The modeling of TWBs by finite elements there are two methods: the first takes into account the weld line (TAZ - Thermally Affected Zone and WZ - Weld Zone), with a much more refined and precise mesh. The second neglects the effects of welding [13]. The first applies only in situations in which there is no localized strain of great intensity in the weld [5,11,14,61,62].

The simplification of the first method may cause a relative discrepancy between the practical and the simulated results. This is because in these models the Tailor Welded Blank Forming Limit Diagram (FLD) is not taken into account, but only the base materials. There is then another challenge to be overcome: prediction of the FLD of a TWB considering the local and global effects of the weld [15,59].

The conventional methods, using stamping software (such as PAMSTAMP®, for example), there is a level of accuracy higher than 94%, which is considered excellent. When working with the stamping of TWBs, this correlation is reduced to 78%, which explains the difficulty in predicting failures [16].

There are several parameters that directly influence the numerical modeling of TWBs. Welding processes can significantly change the mechanical properties of materials in weld zone (WZ) and Heat Affected Zone (HZA). However, materials should not be considered as uniform. To survey the parameters to be adopted in the numerical simulation, the results of experimental tests are necessary, revealing the localized mechanical behavior, such as the flow limit and the plasticity parameters of the regions affected by the welding process [10,11, 5].

The Plasticity is the area of mechanics that relates the calculation of stresses and strains in a body, which needs to be relatively ductile, permanently deformed by a set of applied forces. The theory is based on experimental observations on the macroscopic behavior of metals in uniform states of combined stresses. The results obtained are then idealized in mathematical equations that describe the behavior of metals under complex tensions [17,18,19,5,59].

However, it is necessary to develop more techniques that are experimental and analytical methods to quantitatively assess the mechanical characteristics of the welded metal and the formability of TWBs. Effects such as strain hardening during shaping and anisotropy of welded metal, for example, must be taken into account [20].

For mechanical characterization of Tailor Welded Blanks, tensile tests have been adopted, with specimens of different configurations, to feed numerical simulations and to be confronted with the so-called Mixture Rule [21,22]. In this case, we work with the ASTM E-8M standard [3].

The Mixtures Rule is used to extract properties from the weld, aiming to verify its influence on the mechanical properties and the elongation of the TWB. Thus, the load proportions supported by the weld and the base metal are calculated, assuming homogeneous deformation uniformity for the three materials [3,8].

Than those referred to mechanical effects, we also deal with micro structural issues related to welding in the Weld Zone. The changes, depending on the materials used, can be considerable. It is generated from a local softening of marten site to complex phase transformations in conditions imbalance, depending on the welded materials, the process and the welding parameters [21,23].

The two most used criteria in the numerical modeling of TWBs are based on the Theory of Plasticity: Yield and isotropic hardening. Different models of isotropic hardening in which the plastic deformation largely exceeds the yield, can be used in the modeling of Tailor Welded Blanks [10,11,7]. However, Holloman's equation is the simplest and most widely used model, and can be expressed as:

$$\overline{\sigma} = K\overline{\varepsilon}_p^n \quad (1)$$

Where:

- $\overline{\sigma}$= is the true stress
- K = is the resistance coefficient
- $\overline{\varepsilon}_p$ = is the true strain
- $n$ = is the strain hardening coefficient

After the linearization of the Holloman equation, the strain-hardening coefficient can be determined, which is a key parameter to obtain the maximum deep drawing limit in the inlay operations. The higher the strain hardening coefficient, the greater the capacity of the material to strain, without the occurrence of necking down.

If there is a quantitative relationship between strain rate and yield stress, the Ludwik model can be used, which is a modification of the Holloman equation. In cold work, the yield stress is high at each strain level, mainly due to the strain-hardening phenomenon, so the yield stress is added to the equation [10,11,5]. Ludwik's law can be expressed as:

$$\overline{\sigma} = \sigma_y \; K\overline{\varepsilon}_p^{\,n} \tag{2}$$

Where:

- $\overline{\sigma}$= is the true stress
- $\sigma_y$ = is the yield stress
- $K$ = is the resistance coefficient
- $\overline{\varepsilon}_p$ = is the true strain
- $n$ = is the strain hardening coefficient

The equations can be used so much to forming the TWBs how much for the base metal of the weld. If there is a need to consider the pre-strained material, the Ludwik model can also be modified [10,11,5]. Ludwik's law is modified and can be expressed as the Swift Equation:

$$\overline{\sigma} = \sigma_y \; \mathrm{K}\left(\overline{\varepsilon}_{p+}\overline{\varepsilon}_{0}\right)^{n} \tag{3}$$

Where:

- $\overline{\sigma}$= is the true stress
- $\sigma_y$ = is the yield stress
- $K$ = is the resistance coefficient
- $\overline{\varepsilon}_p$ = is the true strain
- $\overline{\varepsilon}_0$ = is the true strain rate
- $n$= is the strain hardening coefficient

A model widely used in the literature to describe the behavior of metals, such as aluminum, is the Voce equation, which takes into account the three parameters: initial yield stress, maximum stress and relaxation strain in the dynamic recovery regime. Such equation is described as:

$$\overline{\sigma} = \mathrm{A} - \mathrm{Bexp}(-\mathrm{C}\overline{\varepsilon}_{\mathrm{p}}) \tag{4}$$

Where:

- $\overline{\sigma}$= is the true stress
- A= is the steady-state flow stress voltage reached at high deformations
- $\overline{\varepsilon}_p$ = is the true strain
- $C$ = is non-dimensional

For metals such as aluminum and ferritic stainless steels, once recovery is established, its effect is sufficiently efficient to contain hardening strain and the forming stress curve follows a horizontal line. Strains rates for both are omitted in FEM analysis of TWBs. However, one can simply take into account the effect of the strain rate, by multiplying the hardening strain law by a term like $\dot{\varepsilon}^m$ [10,18,24].

Steel sheets, due to the rolling process, have a very significant anisotropy. This can influence data entry for numerical simulation, so it is extremely important to analyze the best yield criterion to be used in experimental tests [24,10,25,26].

However, the importance of anisotropy in the process of forming TWBs, the isotropic criterion of Von Mises and Gurson - Tvergaard - Needleman (GTN) are still frequently used. Von Mises formulated a flow criterion suggesting that this phenomenon occurs when the second invariant of the deviation stresses reaches a critical value. [10,12,26,27]. The Von Mises model can be expressed as:

$$\sqrt{J}_{2\,-\frac{1}{\sqrt{2}}}\Phi\,(\alpha) \tag{5}$$

Where:

- $\Phi$= depends on the hardening strain parameter
- $\alpha$= is the radius of the yield surface

The second invariable tensor is given as:

$$\overline{\sigma} = \sqrt{J_2} \; = \sqrt{3/2}\,S{:}S = \sqrt{3/2\;S_{ij}\,S_{ij}} \; = \; S_{ij} \; = \sigma_{ij} \; - \; \sigma_m \delta_{ij} \tag{6}$$

Where:

- $\overline{\sigma}$= is the equivalent stress
- $\delta_{ij}$ = is the Kronecker delta, in matrix form, corresponds to the identity matrix

Hill's model is proposed for the yield of an anisotropic material and is assumed to be a quadratic function of the stress space. This is can be expressed as:

$$F(\sigma_{22-}\sigma_{23})^2 + G(\sigma_{33-}\sigma_{11})^2 + H(\sigma_{11-}\sigma_{22})^2 + 2L{\sigma_{23}}^2 + 2M{\sigma_{31}}^2 + 2N{\sigma_{12}}^2 = 1 \tag{7}$$

Where:

- $F, G, H, L, M, N$ = are experimentally determined coefficients

The yield surface is defined using the three values r ($r_{0,}r_{45,}r_{90,}$) and the initial yield stress in the rolling direction [10,11,12,25,59]. If the biaxial factor is equal to 1 it is the classic Hill-48 model. Applied to flat tension the criterion can be used as:

$$\sigma_1{}^2 + \frac{R_0(1+R_{90})}{R_0(1+R_0)}\sigma_2{}^2 - \frac{2R_0}{1+R_0}\sigma_1\sigma_2 = \sigma_{y,1}{}^2 \quad (8)$$

Where:

- $\sigma_{y,1}{}^2$ = is the uniaxial yield stress
- $R_0 e\ R_{90}$ = are the coefficients of Lankford

Figure 3 shows how the experimentally extracted anisotropy parameters are related. The RD and TD are the directions in which the test samples of the steel plate are removed. With these parameters, the criteria for numerical simulation of the TWBs are modeled.

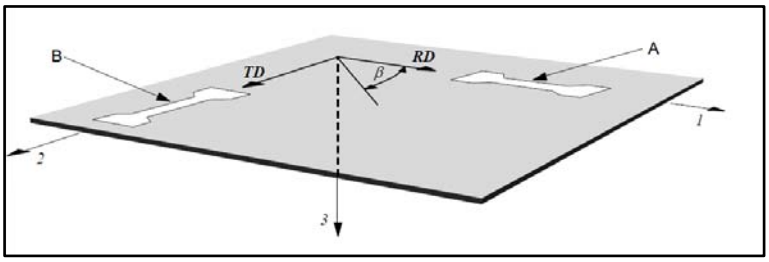


*Source: (Adapted from Theory_of_Plasticity, p.11)*

*Figure 3:* Orientations of the samples plans

The material constants present in the Hill criterion (F, G, H) are related to the parameters experimentally determined RD and TD. for$R_0$we have:

$$R_{\beta=0} = R_0 = \frac{d\varepsilon_{TD}^p}{d\varepsilon_{33}^p} = \frac{d\varepsilon_{22}^p}{d\varepsilon_{33}^p} - \frac{F\sigma_2+H(\sigma_2-\sigma_1)}{F\sigma_2+G\sigma_1} = \frac{H}{G} \quad (9)$$

In case the mode is stretched in the second direction TD, we have the value of$R_{90}$:

$$R_{\beta=90} = R_{90} = \frac{d\varepsilon_{RD}^p}{d\varepsilon_{33}^p} = \frac{d\varepsilon_{11}^p}{d\varepsilon_{33}^p} - \frac{G\sigma_1+(H\sigma_1-H\sigma_2)}{F\sigma_2+G\sigma_1} = \frac{H}{F} \quad (10)$$

In the case of normal anisotropy, the flat stress version of Hill's 1948 yield criterion can be written as:

$$\sigma_1{}^2 + \sigma_2{}^2 - \frac{2R}{1+R}\sigma_1\sigma_2 = \sigma_{y,1}{}^2, R_{90} = R_0 = R_{45} \quad (11)$$

In 1979, Hill proposed a generalized non-quadratic criterion to explain an "anomalous" observation in some aluminum alloys, where the yield forces in biaxial stress were superior to the yield forces in uniaxial stress (which is not allowed by Hill's test 1948) [7,10,12,28]. The proposed model:

$$F|\sigma_2 + \sigma_3|^m + G|\sigma_3 - \sigma_1|^m + H|\sigma_1 - \sigma_2|^m + L|2\sigma_1 - \sigma_2 - \sigma_3|^m + M|2\sigma_2 - \sigma_3 - \sigma_1|^m + N|2\sigma_3 - \sigma_1 - \sigma_2| = \sigma_y{}^m \quad (12)$$

Where:

- $F, G, H, L, M, N$ = are experimentally determined coefficients
- m = can be calculated from the non-linear relationship
- $\sigma_y{}^m$ = is the uniaxial yield stress

Other yield criteria can be derived from this model assuming combinations of experimental parameters [10]. Hosford elaborated his generalized criterion for Hill's yield and can be obtained considering L = N = 0. [10,28]. So for a flat isotropic material we get:

$$\frac{1}{1+R}(|\sigma_1|^m + |\sigma_2|^m) + \frac{R}{R+1}|\sigma_1 - \sigma_2|^m = \sigma_y{}^m \quad (13)$$

Where:

- $\sigma_y{}^m$ = is the uniaxial yield stress
- $R$ = is the coefficient of Lankford

For a non-isotropic material, the Hosford criterion is treated by:

$$G|\sigma_2 - \sigma_3|^m + G|\sigma_3 - \sigma_1|^m + H|\sigma_1 - \sigma_2|^m = 1 \quad (14)$$

Where:

- $F, G, H$ = are the coefficients of Lankford
- m = can be calculated from the non-linear relationship

The Barlat model is formulated in the stress space. The yield surface is defined using the Lankford coefficients ($r_{0,}r_{45,}r_{90,}$) and the exponent m. he Barlat model was specially developed for the description of aluminum alloys. [10.19.28]. It is also a generalization of the Hosford criterion for the case where the directions of the orthotropic axes:

$$\phi = (3I_2)^{\frac{m}{2}}\left\{\left|2\cos\left(\frac{2\theta+\pi}{6}\right)\right|^m + \left|2\cos\left(\frac{2\theta-3\pi}{6}\right)\right|^m + \left|2\cos\left(\frac{2\theta+5\pi}{6}\right)\right|^m\right\} = 2\bar{\sigma}^m \quad (15)$$

Where:

- $\theta$ = $\arccos\left(I2/I3^{3/2}\right)$ with the second and third stress determining invariant ($I_2I_3$) re used using Bishop-Hill notation.
- m = represents the number of experimental r values

The yield model of Gurson Tvergaard Needleman (GTN) are generalizations of two models are the isotropic of Von Mises and Hill 1948 [10,19,26,27,28]. For the isotropic model, we have:

$$\Phi = \left(\frac{\sigma_{eq}}{\sigma_y}\right)^2 + 2q_1\varphi\cos h\left(-q_2\frac{3\sigma_H}{2\sigma_y}\right) - (1+q_3\varphi^2) = 0 \quad (16)$$

Where:

- $\sigma_{eq}$ = is the equivalent stress of Von Mises
- $\sigma_y$ = is the yield stress of material
- $\sigma_H$ = is the Hydrostatic stress of material
- $q_1, q_2, q_{31}$ = are material parameters determined experimentally

For the modified criterion presenting the anisotropy parameters, we have:

$$\Phi = \left(\frac{\sigma_{eq}}{\sigma_y}\right)^2 + 2q_1\varphi \cos h\left(-q_2\sqrt{\frac{1+2R}{6(1+R)}}\frac{3\sigma_H}{\sigma_y}\right) - (1 + q_3\varphi^2) = 0 \quad (17)$$

Where:

- $\sigma_{eq}$ = is the equivalent stress of Von Mises
- $\sigma_y$ = is the yield stress of material
- $\sigma_H$ = is the Hydrostatic stress of material
- $q_1, q_2, q_{31}$ = are material parameters determined experimentally
- R = are the coefficients of Lankford

The numerical simulations used with this criterion are performed to describe the damage to the materials, which involves the triaxiality of the stress, that is, the law is based on the physical ductile fracture mechanism, that is, empty nucleation, growth and coalescence [5,7,10,19,26, 28].

## IV. Finite Elements Method for Modeling of TWBs

One of the main objectives in applying a virtual analysis (figure 4) is to calculate the movement of the weld line and provide an ideal force balance between the punch and blankholder. The results of this combination aim to control the flow of the blank to be forming, avoiding the movement of the weld line and thus reducing the high tensile stresses perpendicular to the weld line [29,61,62,55].

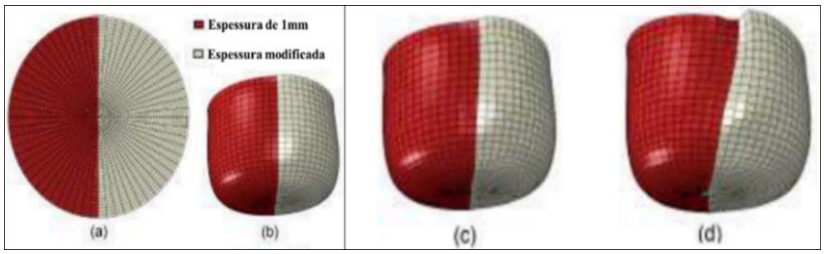


*Source: (Adapted from FAZLI, 2016).*

a) initial blank b) thicknesses of 0.85mm and 1mm c) thicknesses of 0.75mm and 1mm d) thicknesses of 0.5mm and 1mm.

*Figure 4:* Initial blank and three samples stamping with different thickness combinations

As the weld line moves to critical deep areas of inlay, the forming of the blank decreases. In some studies developed to control this situation, several tests have been carried out to decrease the strain in the thicker material, from increasing the flow of the thicker material and even reducing the stamping force on the thinner material. For that, the concept of draw beads was worked and pressure points were controlled in isolated quadrants of the blank holder [1,61,62].

Adony and Chen cited by Gautam found a strong correlation between the ductility of the weld and the limiting dome height for longitudinally welded TWBs, doing flat stretch, with original materials of similar thickness and different materials and coating combinations. The Limiting Drawing Ratio (LDR) for a TWB is between the values of the thinnest and thickest sheet if the thickness ratio is different from the unit [30,31].

According to research carried out by R. Safdarian and M. J. Torkamany, he describes that after the experimental tests carried out; the different thicknesses of the TWBs were modeled in the ABAQUS® program. The Finite Elements Method (FEM) was used to construct Forming Limit Diagram (FLD) based on the Hecker principle. In the physical cupping tests, the Limit Dome Height parameter was used, as shown in figure 5 [25].

For simulation, the following data were collected from the materials that make up the TWB: Yield Strength (YS), Ultimate Tensile Strength (UTS), hardening exponent (n), hardening coefficient (K) , total elongation and anisotropy coefficient ($R_0$, $R_{45}$, $R_{90}$) [25].

In the modeling, the Punch, Die and blankholder were considered as rigid items. The TWBs were modeled as a shell element with S4R elements, maintaining the left and right side weld line inclination between 20 ° and 45 °. The calculation of stresses and strains was based on the Hill criterion (1948) and a flat state of strain was sought. To perform the tests, the use of a 20-ton hydraulic press is suggested [25].

The experimental results show that the greater the difference in thickness and mechanical strength between the materials that make up the TWB, the greater the movement of the weld line. As a consequence, the lower the stamping of the TWB will be, which is reflected in a lower Limit Dome Height (LDH), as shown in figure 5 [25].

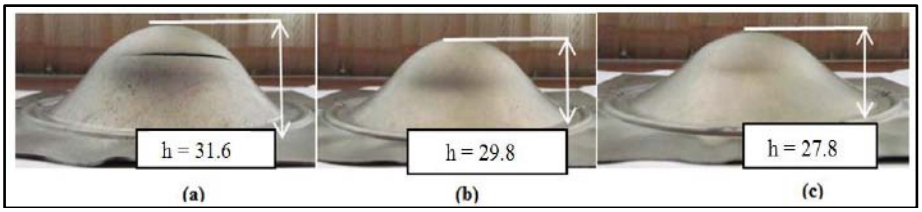


Source: Safdarian; Torkamany, 2016

*Figure 5:* Limit Dome Height for different thickness ratios (A) 1.25 (B) 1.7 and (C) 2.13

Figure 6 shows the movement of the weld line in mm, due to the reason for different thicknesses after the experiments.

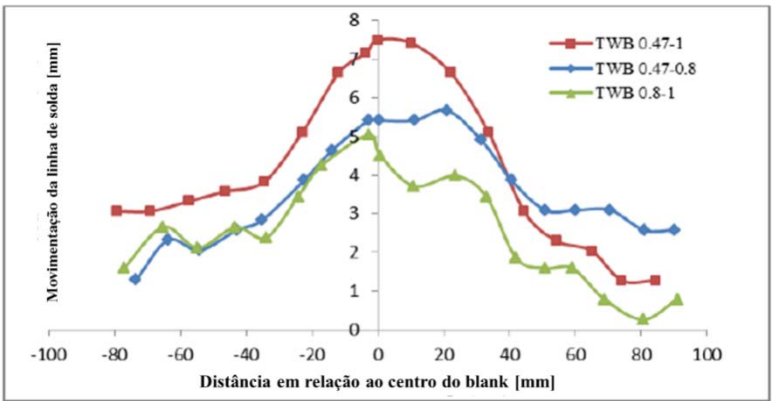


Source: Safdarian; Torkamany, 2016

*Figure 6:* Movement of the weld line for different thickness ratios of the plates that make up the TWB

In general, the greater the difference in thickness and mechanical strength between the materials that make up the TWB, the greater the movement of the weld line. Consequently, less tends to be its conformability [25].

According to research by Masumi, Nakajimacupping tests, tensile tests and simulations were performed to correlate the values obtained experimentally. In the simulations, the effects of welding on WZ and HAZ were not considered. The weld line was referred to only as the dividing point between the two materials that made up the TWB. For a better correlation, it was necessary to use the anisotropy criteria and parameters [5,32].

In the work developed by Gautam, for the TWB, the simulation was performed on half the blank, being obtained for a complete blank using the principle of symmetry on the X-Y plane, this is technique was applied to reduce the size of the problem and the time of the simulation. The FEM analysis of the base material sheet was also performed to compare the LDH values obtained in each case [30,31].

Hill's plasticity model, also known as Hill's yield potential, which is an extension of the Von Mises function for anisotropic materials, was used in finite element modeling to incorporate sheets anisotropy.

Figure 7 shows the mesh and elements used for simulation in Gautam's work.

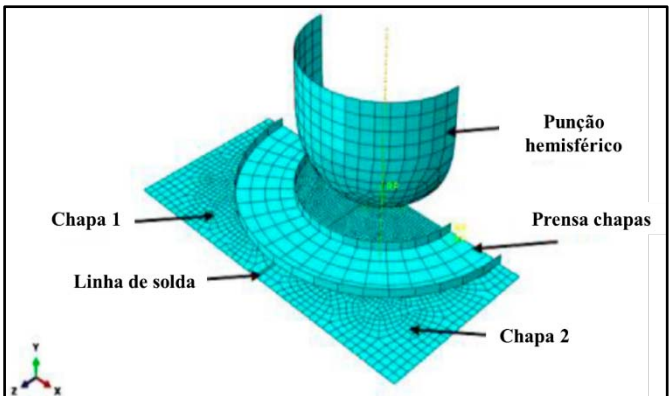


Source: Adapted from Gautam et al (2019).

*Figure 7:* Mesh and elements used for simulating a TWB

Gautam's experimental results showed that LDH is higher in the thicker sheet than in the less thick sheet, indicating greater formability of the thicker sheet. Similar results were observed in the simulations, although higher LDH values were obtained in a simulated manner [30,31].

The refinement of simulations through experimental tests is of fundamental importance. The failure points predicted for the FLD were captured in the DYNAFORM® software. These points were plotted as major and minor strains for a comparison with the actual stress data obtained from the LDH experiments [30,31].

Gautam's results showed that the simulation predicts a maximum displacement value of the weld line of 2.45mm, which is lower than the experimental values of 2.57mm. This deviation in the results of the displacement of the weld line obtained by experiments and the numerical results can be attributed to the friction between the punch and the blank [30,31].

In another study, developed by Korouyeh in interstitial free steel sheets (IF - Interstitial Free) were used to compose a TWB. The numerical investigation of the TWBs forming was done using a commercially available finite element code ABAQUS 6.10® [60].

The model consisted of a hemispherical punch, blankholder, die and blank. This model was based on the Hecker Forming Limit Diagram (FLD) test. Eight specimens of size 25mmx200mm to 200mmx200mm were cut from the laser-welded sample, so that the weld line was perpendicular to the stretch direction (cross-sectional samples) [33].

In the standard cupping tests, the check also took place on the thinner side of the TWB and parallel to the weld line. Figure 8 shows the FLD of the TWB made. It is noticed that the numerical criteria cannot predict the right side of the FLD, being suitable only for the left side, under condition of plane strain.

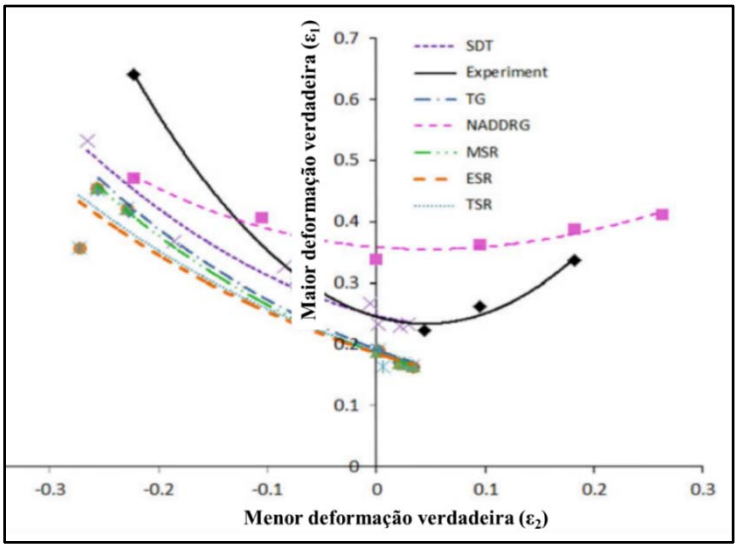


*Source: Korouyeh et al, 2012.*

*Figure 8:* Different FLDs from the same TWB, obtained from different methods

Figure 9 shows the results for samples of different widths, showing that there are different heights of LDH. For experiments and numerical criteria, the LDH height was smaller for the 125mm wide sample.

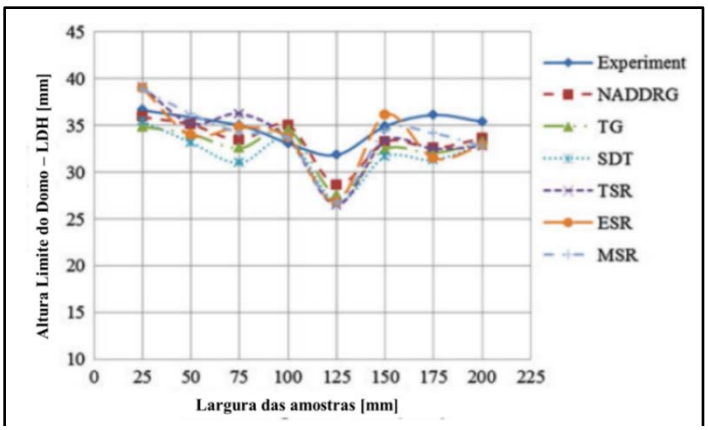


*Source: Korouyeh et al, 2012.*

*Figure 9:* Results of the LDH test, for samples of different widths, working with different evaluation criteria

TWB samples with different widths produce different LDH values, so the dispersion of the LDH test depends on the variation of the stress path at the fracture site. For experiments and numerical criteria, the LDH value is minimum for a 125mm wide sample that is in the plane stress condition [33].

The comparison of the fracture position of the FEM and the experiment shows that there is good agreement for the fracture position predicted by the SDT criterion and experiment. The results show that, due to the increase of the sample width or in the condition of biaxial elongation, the fracture occurs closer to the weld line.

In research carried out by Andrade and Santos, the conditions found to be optimal in the tensile test (relative inclination of the 30º and 60º weld line) were simulated. In this work, it was evidenced that the total relative elongation of the weld line would support a maximum strain for an angle of 30 ° in relation to the rolling direction of the base materials. The AutoForm® forming software, from the AutoForm ®Company with triangular meshes, Shell model, friction coefficient 0.15 was used. The materials considered were FEE 210 with 1.10mm and FeP05 0.65mm, both IF. The yield criterion used was based on the Hill 1948 and the Hollomon model [2,3,8,34].

Figure 10 Represents the maximum elongation graph extracted in the tensile test for an angle of 30 °

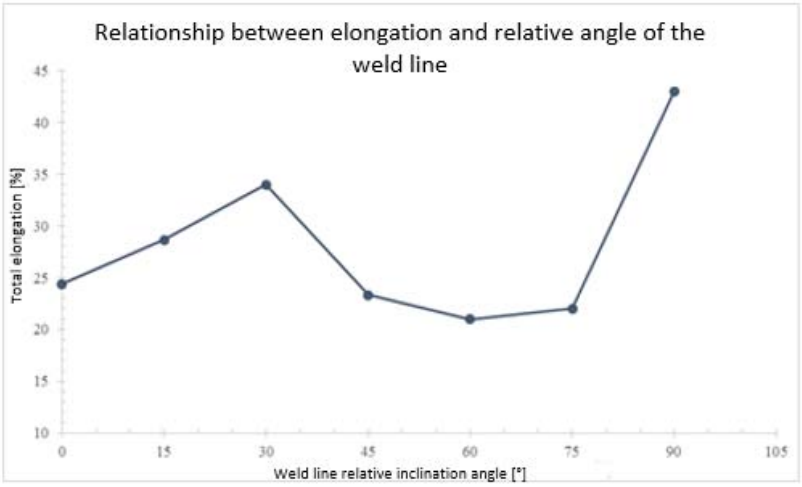


*Source: Andrade, Etiene Pereira de; Santos, Wellington Augusto dos, 2019.*

*Figure 10:* Relationship between the total elongation and the relative inclination angle of the weld line

After the experimental test, the Door Inner was simulated as shown in figure 10. That product always presented several stamping problems, such for example as localized splits in deep-drawn part.

Figure 11 Result of the stamping simulation, showing strain deviation curve as a function of the relative inclination angle of the weld line

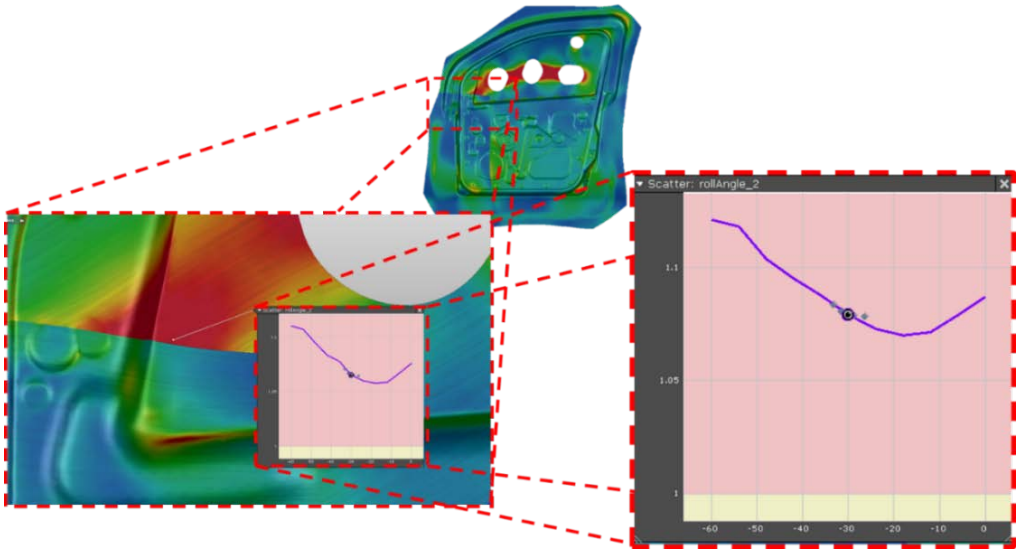


*Source: Andrade, Etiene Pereira de Santos, Wellington Augusto dos, 2019.*

*Figure 11:* Result of the stamping simulation

According to the highlighted strain curve, it turns out that the maximum stress peak tends to decrease, indicating that the purely tensile stresses are attenuated. Even that happen the weld line fractures, efforts will are reduced. This indicates the relative improvement in mechanical behavior when tilting the weld line. However, the simulation does not take into account the weld (HAZ and WZ), nor their mechanical properties [2,3,5,8,34].

In summary, there is then a lack of methods and processes that more accurately determine the effects of the forming about the TWB. It is therefore necessary to develop more experimental techniques and analytical methods to quantitatively evaluate the mechanical characteristics of the welded metal and the formability of TWBs. Effects such as hardening strain during shaping and anisotropy of welded metal, for example, must be taken into account. In this respect, the use of simulations is will growing and aims to overcome the challenges mentioned above.

## V. Conclusions

A review of the TWBs was elaborate and in most of the work done, researchers always adopt a numerical model in their studies that disregards the WZ and the HAZ. This parameter is often adopted due to the limitations of the software's used, due to the high computational cost or the lack of experimental data for the mechanical and micro structural behavior of the weld.

Usually the elements of numerical analysis used are the shell, due to its speed of data processing and good precision. However, the inclusion of the Heat-Affected Zone (modeled also by the shell element) does not represent an improvement in the results forming and the localized Springback\ effect. The reason is that due greater resistance to yield and Heat-Affected Zone modulus of the weld has an opposite effect to the elastic return.

An alternative likely would be to model the weld in 3D solid elements and the base materials by the shell element. Where the movements of the dependent nodes will be interpolated from the movement of independent nodes in the base metal mesh. The solid formulation in the region is the case where the elastic portion of the deformation is not neglected.

However, to that, there is a good approximation for numerical modeling, some conclusions are recommended:

- ✓ Previous qualification and analysis of the weld, by means of microscopy, either optical or electron beam scanning;
- ✓ The weld line must not be worked entirely parallel to the rolling direction (relative inclination of 0°), nor entirely perpendicular (relative inclination of 90°), as it tends to facilitate the propagation of cracks, splits and worsen the mechanical behavior of the TWB;
- ✓ It is necessary that the base materials work in a balance of forces (FA = FB) and, to satisfy these conditions, disregarding the metallurgical effects. This thickness ratio, the greater than the unit (1.0), the worse the forming, the threshold can be obtained by the equation: $\mathrm{LSR} = \left(\frac{\sigma_{YB}}{\sigma_{TA}}\right) = \left(\frac{t_{0A}}{t_{0B}}\right)$(18)
- ✓ The tensile tests, once the weld is qualified, proved to be useful for surveying the mechanical properties of the TWB and the influence of the relative inclination of the weld line on its performance during forming;
- ✓ Determination of an optimized curve (FLD) for the three materials, including here the weld region , which is extremely important for the development of TWBs, because with the obtaining of the curve it is possible to previously identify conditions that would lead to plastic instability or even to material failure.

The validation of the numerical model requires constant comparison with experimental results, in order to identify possible deviations in the simulation results. Thus, the validation of numerical simulation has a fundamental role in this field of investigation.

## Acknowledgments

The authors would like to thank FIAT Chrysler do Brazil for the technical contribution to this research, Capes (Coordination for the Improvement of Higher Weight) and PUC Minas (Pontifical Catholic University of Minas Gerais) for financially supporting this research and for assisting in the publication of this article.

## References Références Referencias

1. MEINDERS, T; BERG, A Van Den; HUÉTINK, J. Deep drawing simulations of Tailor Blanks and experimental verification. Journal of Materials Processing Technology, [s.l.], v. 103, n. 1, p.65-73, jun. 2000. Elsevier BV.
2. ASSUNÇÃO, Guilherme Souza; ANDRADE, Etiene Pereira de; SANTOS, Wellington Augusto dos; FELIZARDO, Ivanilza Felizardo; BRACARENSE, Alexandre Queiroz Bracarense. Caracterização Mecânica da Região Soldada de Tailor Welded Blanks (TWB) a Partir do Perfil de Microdureza. Soldagem & Inspeção, [s.l.], v. 24, p.1-10, 2019. FapUNIFESP (SciELO). http://dx.doi.org/10.1590/0104-9224/si24.32.
3. ANDRADE, Etiene Pereira de; ASSUNÇÃO, Guilherme Souza; SANTOS, Wellington Augusto dos; FELIZARDO, Ivanilza Felizardo; BRACARENSE, Alexandre Queiroz Bracarense. Caracterização Mecânica e Análise Microestrutural de Chapas Obtidas pelo Processo de Tailor Welded Blank (TWB). Soldagem & Inspeção, [s.l.], v. 24, p.1-11, nov. 2019. FapUNIFESP (SciELO). http://dx.doi.org/10.1590/0104-9224/si24.25

4. ZADPOOR, A. A., Sinke , J. and Benedictus , R. (2008 a) ' Experimental and numerical study of machined aluminum tailor made blanks ', Journal of Materials Processing Technology ,200 , 288 – 299.
5. M. Shehryar Khan, M. H. Razmpoosh, E. Biro & Y. Zhou (2020): A review on the laser welding of coated 22MnB5 press-hardened steel and its impact on the production of tailor-welded blanks, Science and Technology of Welding and Joining, 26 Mar 2020.https://doi.org/10.1080/13621718.2020.1742472.
6. DOS REIS, L.C.: Estudo dos Parâmetros de Influência na simulação numérica de estampagens de Chapas. Dissertação de Mestrado. Curso de Pós-Graduação em Engenharia Metalúrgica e de Minas. UFMG. 2002.
7. Amit Kumar Rana; Suchibrata Datta; Sanjib Kundu. Deformation behaviour during deep drawing operation under simple loading path: A simulation study, [s.1], V. 2; n.3, p. 1–6, 31 December 2019. Elsevier BV. https://doi.org/10.1016/j.matpr.2019.12.413
8. ANDRADE, Etiene Pereira de SANTOS, Wellington Augusto dos; BRACARENSE, Alexandre Queiroz. Caracterização mecânica e análise de falhas de chapas fabricadas pelo processo de Tailor Welded Blank submetidas a estampagem profunda. ABM Proceedings, [s.l.], p.293-301, out. 2017. Editora Blucher.
9. AUTOFORM PLUS R3.1®: Software for Sheet Metal Forming. AutoForm Engineering GmbH.2011.
10. ZADPOOR, A. A,; SINKE, J,; BENEDICTUS,R. Woodhead Publishing Limited, 2011 Numerical simulation modeling of tailor welded blank forming. Materials Innovation Institute (M2i) and Delft University of Technology, the Netherlands:p.68-94, 2011Woodhead Publishing Limited.
11. Yong Chan Hur; Yong Chan Hur; Byung Min Kim; Myoung-Gyu; Ji Hoon Kim. MEASUREMENT OF WELD ZONE PROPERTIES OF LASER-WELDED TAILOR-WELDED BLANKS AND ITS APPLICATION TO DEEP DRAWING. 2020 KSAE/ 115–08 pISSN, [s.1], V. 21; n.3, p. 615–622, 30 January 2019. International Journal of Automotive Technology. https://DOI 10.1007/s12239–020–0058.
12. Hossein Moayedi; Roya Darabi; Aria Ghabussi; Mostafa Habibi; Loke Kok Foong h. Weld orientation effects on the formability of tailor welded thin steel sheets, ScienceDirect ,[s.1],V. 21; n.3, p. 615–622 15 February 2020. Elsevier BV. https://doi.org/10.1016/j.tws.2020.106669.
13. WANG, H.; ZHOU, J.; ZHAO, T.S.; LIU, L.Z.; LIANG, Q. et al. Multiple-iteration spring back compensation of tailor welded blanks during stamping forming process. Materials & Design, [s.l.], v. 102, p.247-254, jul. 2016.
14. SHI, Ming F.; PICKETT, Ken M.; BHATT, Kumar K.. Formability Issues in the Application of Tailor Welded Blank Sheets. Sae Technical Paper Series, [s.l.], p.1-11, 1 mar. 1993. SAE International.
15. PANDA, Sushanta Kumar; KUMAR, D. Ravi; KUMAR, Harish; NATH, A.K.. Characterization of tensile properties of tailor welded IF steel sheets and their formability in stretch forming. Journal Of Materials Processing Technology, [s.l.], v. 183, n. 2-3, p.321-332, mar. 2007. Elsevier BV.
16. KARAJIBANI, Ehsan; HASHEMI, Ramin; SEDIGHI, Mohammad. Determination of forming limit curve in two-layer metallic sheets using the finite element simulation. Proceedings of the Institution of Mechanical Engineers, Part L: Journal of Materials, [s.l.], v. 230, n. 6, p.1018-1029, 3 ago. 2016. SAGE Publications.
17. BRESCIANI FILHO, Ettore et al. Conformação Plástica Dos Metais. 6. ed. Campinas: Epusp, 2011. 254p.
18. DIETER, G. E. Mechanical metallurgy. 3 Ed. Boston: McGraw-Hill, 1988.
19. https://www.researchgate.net/publication/329680368_Theory_of_Plasticity [accessed Dec 08 2019]
20. KIM, Jaehun; KIM, Sanseo; KIM, Keunug; JUNG, Wonyeong; YOUN, Deokhyun; LEE, Jangseok; KI, Hyungson. Effect of beam size in laser welding of ultra-thin stainless steel foils. Journal Of Materials Processing Technology, [s.l.], v. 233, p.125-134, jul. 2016. Elsevier BV
21. KHAN, Arman; SURESH, V.V.N.Satya; REGALLA, Srinivasa Prakash. Effect of Thickness Ratio on Weld Line Displacement in Deep Drawing of Aluminium Steel Tailor Welded Blanks. Procedia Materials Science, [s.l.], v. 6, p.401-408, 2014. Elsevier BV.
22. SURESH, V. V. N. Satya; REGALLA, Srinivasa Prakash; GUPTA, Amit Kumar. Combined effect of thickness ratio and selective heating on weld line movement in stamped tailor-welded blanks. Materials And Manufacturing Processes, [s.l.], v. 32, n. 12, p.1363-1367, 10 nov. 2016. Informa UK Limited.
23. CALLISTER, William D.; RETHWISCH, David G.. Ciência e Engenharia de Materiais: Uma Introdução. 9. ed. São Paulo: LTC: GEN - Grupo Editorial Nacional, 2016. 912 p.
24. CETLIN, PR; HELMAN, H. Fundamentos da conformação: mecânica dos metais. 2. ed. São Paulo: Artliber; 2005. 265 p.
25. SAFDARIAN, R. The effects of strength ratio on the forming limit diagram of tailor-welded blanks. Ironmaking & Steelmaking, [s.l.], v. 45, n. 1, p.17-24, 27 set. 2016. Informa UK Limited.
26. Abdelkader, Slimane,; Benattou Bouchouicha,; Mohamed Benguediab,; Sid-Ahmed Slimaneb, 2015 Parametric study of the ductile damage by the

Gurson–Tvergaard–Needleman model of structures in carbon steel A48-AP. Brazilian Metallurgical, Materials and Mining Association: v. 4, n. , p.2017-223, 2015. Elsevier BV.

27. Safdarian, R., "Forming Limit Diagram Prediction of AISI 304–St 12.Tailor Welded Blanks Using GTN Damage Model," Journal of Testing and Evaluation, [s.1], V.2, n.1, p.1-16, January 15, 2019. ASTM International. https:// doi.org/10.1520/JTE20180069.
28. HOSFORD, William F.; CADDELL, Robert M.. Metal Forming: Mechanics and Metallurgy. 3. ed. Nova Iorque: Cambridge University Press, 2007. 312 p.
29. KINSEY, Brad L.; WU, Xin. Tailor welded blanks for advanced manufacturing. Cambridge: Woodhead Publishing Limited, 2011. 217 p.
30. GAUTAM, Vijay; RAUT, Vinayak Manohar; KUMAR, D Ravi. Analytical prediction of spring back in bending of tailor-welded blanks incorporating effect of anisotropy and weld zone properties. Proceedings of the Institution of Mechanical Engineers, Part L: Journal of Materials, [s.l.], v. 232, n. 4, p.294-306, 4 jan. 2016. SAGE Publications.
31. GAUTAM, Vijay; KUMAR, Arvind. Experimental and Numerical Studies on Formability of Tailor Welded Blanks of High Strength Steel. Procedia Manufacturing, [s.l.], v. 29, p.472-480, 2019. Elsevier BV.
32. MAMUSI, Hossein; MASOUMI, Abolfazl; HASHEMI, Ramin; MAHDAVINEJAD, Ramazanali. A Novel Approach to the Determination of Forming Limit Diagrams for Tailor-Welded Blanks. Journal of Materials Engineering and Performance, [s.l.], v. 22, n. 11, p.3210-3221, 27 jun. 2013. Springer Nature
33. KOROUYEH, R. Safdarian; NAEINI, H. Moslemi; TORKAMANY, M.J.; LIAGHAT, Gh.. Experimental and theoretical investigation of thickness ratio effect on the formability of tailor welded blank. Optics & Laser Technology, [s.l.], v. 51, p.24-31, out. 2013. Elsevier BV.
34. ANDRADE, Etiene Pereira de. Caracterização mecânica e análise microestrutural de chapas obtidas pelo processo de Tailor Welded Blank (TWB). 2019. 115 f. Dissertação (Mestrado) - Curso de Engenharia Mecânica, PPGMEC, Universidade Federal de Minas Gerais, Belo Horizonte, 2019.
35. ABDULLAH, K.; WILD, P.M.; JESWIET, J.J.; GHASEMPOOR, A. Tensile testing for weld deformation properties in similar gage tailor welded blanks using the rule of mixtures. Journal Of Materials Processing Technology, [s.l.], v. 112, n. 1, p.91-97, maio 2001. Elsevier BV.
36. AFFONSO, Luiz Otávio Amaral. Ductile and Brittle Fractures. In: AFFONSO, Luiz Otávio Amaral. Machinery Failure Analysis Handbook: Sustain Your Operations and Maximize Uptime. Houston: Gulf Publishing Company, 2007. Cap. 4. p. 33-42.
37. AMERICAN SOCIETY FOR TESTING AND MATERIALS. ASTM E8/E8M: Standard Test Methods for Tension Testing of Metallic Materials. 16 ed. West Conshohocken: ASTM International, 2016. 30 p.
38. ANDRADE, Etiene Pereira de: Estudo do Efeito das Condições de Processamento Mecânico na Transformação de fases do aço inoxidável AISI - Centro Federal de Educação Tecnológica de Minas Gerais, Belo Horizonte, 2015.
39. ASSUNÇÃO, Eurico; QUINTINO, Luisa; MIRANDA, Rosa. Comparative study of laser welding in tailor blanks for the automotive industry. The International Journal of Advanced Manufacturing Technology, [s.l.], v. 49, n. 1-4, p.123-131, 17 nov. 2009. Springer Nature.
40. BROWN, Arthur A.; BAMMANN, Douglas J.. Validation of a model for static and dynamic recrystallization in metals. International Journal of Plasticity, [s.l.], v. 32-33, p.17-35, maio 2012. Elsevier BV. http://dx.doi.org/10.1016/j.ijplas.2011.12.006.
41. CASTRO, Frederico de Magalhães: Estudo Numérico e Analítico das Evoluções da Força e da Espessura em Chapas de Aço Livre de Intersticiais Durante Processamento por Embutimento e Ironing. 2005. 63 f. Dissertação (Mestrado) – Universidade Federal de Minas Gerais, Belo Horizonte, 2005.
42. DHARAN, C. K. H.; KANG, B. S.; FINNIE, Iain. Cleavage and Ductile Fracture Mechanisms: The Microstructural Basis of Fracture Toughness. In: DHARAN, C. K. H.; KANG, B. S.; FINNIE, Iain. Finnie's Notes on Fracture Mechanics: Fundamental and Practical Lessons. Nova Iorque: Springer, 2016. Cap. 7. p. 201-213.
43. DUAN, Libin; XIAO, Ning-Cong; LI, Guangyao; XU Fengxiang; CHEN, Tao; CHENG, Aiguo. Bending analysis and design optimization of tailor-rolled blank thin-walled structures with top-hat sections. International Journal Of Crashworthiness, [s.l.], v. 22, n. 3, p.227-242, 8 nov. 2016. Informa UK Limited.
44. FAZLI, Ali. Investigation of The Effects of Process Parameters on The Welding Line Movement in Deep Drawing of Tailor Welded Blanks. International Journal of Advanced Design and Manufacturing Technology, [s.l.], v. 9, n. 2, p.45-52, abr. 2016. TWB.
45. GONG, Hongying; WANG, Sifan; KNYSH, Paul; KORKOLIS, Yannis P.. Experimental investigation of the mechanical response of laser-welded dissimilar blanks from advanced- and ultra-high-strength steels. Materials & Design, [s.l.], v. 90, p.1115-1123, jan. 2016. Elsevier BV.
46. HE, Sijun; WU, Xin; HU, S. Jack. Formability Enhancement for Tailor-Welded Blanks Using Blank Holding Force Control. Journal of Manufacturing

Science and Engineering, [s.l.], v. 125, n. 3, p.461-467, 2003. ASME International.
47. INTERNATIONAL ORGANIZATION FOR STANDARDIZATION. 6892-1: Metallic materials — Tensile testing — Part 1: Method of test at room temperature. 2 ed. Geneva: ISO, 2016. 79 p.
48. KOROUYEH, R. Safdarian; NAEINI, H. Moslemi; TORKAMANY, M.J.; LIAGHAT, Gh.. Experimental and theoretical investigation of thickness ratio effect on the formability of tailor welded blank. Optics & Laser Technology, [s.l.], v. 51, p.24-31, out. 2013. Elsevier BV.
49. LEE, Dong Nyung; KIM, Yoon Keun. On the rule of mixtures for flow stresses in stainless-steel-clad aluminium sandwich sheet metals. Journal Of Materials Science, [s.l.], v. 23, n. 2, p.558-564, fev. 1988. Springer Science and Business Media LLC. http://dx.doi.org/10.1007/bf01174685.
50. LI, J.; NAYAK, S.S.; BIRO, E.; PANDA, S.K.; GOODWIN, F.; ZHOU, Y. Effects of weld line position and geometry on the formability of laser welded high strength low alloy and dual-phase steel blanks. Materials & Design (1980-2015), [s.l.], v. 52, p.757-766, dez. 2013. Elsevier BV
51. LI, Guangyao; XU, Fengxiang; HUANG, X.; SUN, Guangyong. Topology Optimization of an Automotive Tailor-Welded Blank Door. Journal Of Mechanical Design, [s.l.], v. 137, n. 5, p.055001-055008, 5 mar. 2015. ASME International.
52. LI, Yanhua; LIN, Jianping. Experimental and Numerical Investigations of Constraint Effect on Deformation Behavior of Tailor-Welded Blanks. Journal of Materials Engineering and Performance, [s.l.], v. 24, n. 8, p.2957-2969, 30 jun. 2015. Springer Nature.
53. LIU, Jun; WANG, Li-Liang; LEE, Junyi; CHEN, Ruili; EL-FAKIR, Omer; CHEN, Li; LIN, Jianguo; DEAN, Trevor A.. Size-dependent mechanical properties in AA6082 tailor welded specimens. Journal of Materials Processing Technology, [s.l.], v. 224, p.169-180, out. 2015. Elsevier BV.
54. MERKLEIN, Marion; JOHANNES, Maren; LECHNER, Michael; KUPERT, Andreas. A review on tailor blanks—Production, applications and evaluation. Journal of Materials Processing Technology, [s.l.], v. 214, n. 2, p.151-164, fev. 2014. Elsevier BV.
55. Miguel A. Sanz,; K. Nguyen,; Marcos Latorre,; Manuel Rodríguez,; Francisco J. Montáns. Sheet metal forming analysis using a large strain anisotropic multiplicative plasticity formulation, based on elastic correctors, which preserves the structure of the infinitesimal theory. Finite Elements in Analysis and Design v. 164, n. 1, p.1-17, 2019. Elsevier BV.
56. MIYAZAK, Yasunobu; SAKIYAMA, Tatsuya; KODAMA, Shinji. NIPPON Steel Technical Report: Welding Techniques for Tailor Blanks. 95. ed. Japão (Tóquio): NSSM, 2007. 7 p.
57. NALLI, F.; SPENA, P. Russo; CORTESE, L.; REITERER, D.. Global-local characterization and numerical modeling of TWB laser welded joints. In: International Mechanical Engineering Congress and Exposition - IMECE, 5., 2017, Flórida (Tampa). Proceedings of the ASME 2017 International Mechanical Engineering Congress and Exposition. Flórida (Tampa): ASME, 2017. p. 1 - 8.
58. RIAHI, M; AMINI, A.; SABBAGHZADEH, J.; TORKAMANI, M.J.. Analysis of weld location effect and thickness ratio on formability of tailor welded blank. Science and Technology of Welding and Joining, [s.l.], v. 17, n. 4, p.282-287, maio 2012. Informa UK Limited.
59. SCHREK, A.; ŠVEC, P.; BRUSILOVÁ, A.. Formability of Tailor-Welded Blanks From Dual-Phase and Bake-Hardened Steels with a Planar Anisotropy Influence. Strength Of Materials, [s.l.], v. 49, n. 4, p.550-554, jul. 2017. Springer Nature.
60. SINGH, Mayank Kumar. Application of Steel in Automotive Industry. International Journal of Emerging Technology and Advanced Engineering, [s.l.], v. 6, n. 7, p.246-253, jul. 2016
61. VIJAY, GAUTAM.; ARVIND KUMAR. Experimental and Numerical Studies on Formability of Tailor Welded Blanks of High Strength Steel. 18th International conference on Sheet Metal, v.29, n.1, p472-480, feb.2019. Elsevier BV.
62. Won-Ik, CHO.; PEER WOIZESCHKE.; VILLADS SCHULTZ. Simulation of molten pool dynamics and stability analysis in laser buttonhole welding.10th CIRP conference on Photonic Technologies, v. 74, n. 1,p.687-690, 2018.Elsevier BV.
63. Yanhong Um,; Jing Zhou,; Baoyu Wang,; Qiaoling Wang,; Andrea Ghiotti,; Stefania Bruschi,; Numerical simulation of hot stamping by partition heating based on advanced constitutive modelling of 22MnB5 behaviour. Finite Elements in Analysis and Design, v. xxx, n. 1, p.1-11, 2018. Elsevier BV.
64. ZADPOOR, Amir Abbas; SINKE; Jos; BENEDICTUS, Rinze; PIETERS, Raph. Mechanical properties and microstructure of friction stir welded tailor-made blanks. Materials Science And Engineering: A, [s.l.], v. 494, n. 1-2, p.281-290, out. 2008. Elsevier BV.
65. ZHAO, K.M; CHUN, B.K; LEE, J.K. Finite element analysis of tailor-welded blanks. Finite Elements in Analysis and Design, [s.l.], v. 37, n. 2, p.117-130, fev. 2001. Elsevier BV.
66. G.D. Huynh; X. Zhuang; H.G. Bui; G. Meschke; H. Nguyen-Xuan.Elasto-plastic large deformation analysis of multi-patch thin shells by is geometric approach. Finite Elements in Analysis and Design, [s.l.], v. 3, n. 2, p.1-12, fev. 2020. Elsevier BV. https://doi.org/10.1016/j.finel.2020.103389.